Single station estimation of earthquake early warning parameters by using amplitude envelope curve

Parisa Hosseini[1], Reza Heidari[2*], and Noorbakhsh Mirzaei[3]

[1]*M. Sc., Department of Geophysics, Science and Research Branch, Islamic Azad University, Tehran, Iran*
[2]*Assistant Professor, Department of Earth Sciences, Science and Research Branch, Islamic Azad University, Tehran, Iran*
[3]*Professor, Institute of Geophysics, University of Tehran, Tehran, Iran*

(Received: 28 February 2018, Accepted: 09 July 2018)

Abstract

In this study, new empirical relationships to estimate key parameters in Earthquake Early Warning (EEW) system including magnitude, epicentral distance and Peak Ground Acceleration (PGA) are introduced based on features of the initial portion of P-wave's amplitude envelope curve.

For this purpose, 226 time series recorded by bore-hole accelerometers of Japanese KiK-net are processed for earthquakes with magnitudes from 3 to 7.2 M_{JMA} and epicentral distances of less than 50 km. Hereby, an improved single station method for estimation of epicentral distance and two new methods for estimation of magnitude and amplitude of PGA are proposed based on exponentially envelope curve as $B \times t \times e^{-A \times t}$ in known (B – Δ) method. A scaling relationship of $B \times T_r - \Delta$ is proposed to estimate epicentral distance which is well correlated for larger earthquakes ($M > 6$), with results more robust and reliable than the previous method (B – Δ). Non-dimensional parameter, T_r depends on earthquake magnitude and A parameter in the above-mentioned function. By using the features of acceleration envelope curve and peak amplitude of P-waves, scale parameter S_a is proposed that is well correlated with magnitude and has capability of estimating magnitude with standard deviation of less than ± 0.77 magnitude unit. S_a is proportional to a part of area under envelope curve as a function of magnitude. Moreover, it is indicated that PGA in a single station can be estimated by using envelope curve characteristics of initial P-waves portion.

Keywords: earthquake magnitude, envelope, B – Δ, earthquake early warning system, epicentral distance, peak ground acceleration.

[*]Corresponding author: r.heidari61@gmail.com

1 Introduction

EEW systems are established in order to reduce human and financial losses caused by destructive earthquakes. Nowadays, an efficient EEW system should be capable of timely and correctly recognition of an earthquake, precise magnitude, epicentral distance and amplitude of strong ground motions estimation in areas around fault zones and areas distant from the earthquake epicenter, and issuing warning whenever the earthquake can be destructive. In recent decades, with development of global and local networks, and modern methods for data processing and collecting information from real-time processing, EEW systems have been significantly promoted throughout the world and in some countries have been implemented with high seismicity potential such as Japan (Nakamura 1988, 2004; Kamigaichi, 2004; Kamigaichi et al., 2009; Horiuchi et al., 2005; Hoshiba et al., 2011), Mexico (Espinosa-Aranda et al., 1995, 2009) and Taiwan (Wu and Teng, 2002; Wu and Zhao, 2006).

In general, there are two types of EEW systems: regional early warning systems and the on-site ones. In the first case, a network of seismometers and accelerometers are installed near fault zones to receive the seismic wave phases. These fault areas are located away from the target areas. Upon the occurrence of an earthquake, seismic source parameters (including magnitude and location of the earthquake) from the recorded initial portion of P-waves are evaluated at least in three or four stations, then, the earthquake intensity in target points is estimated by using the attenuation relations (Satriano et al., 2010; Kuyuk and Allen, 2014). In the on-site method, after initial P-waves portion are received by a sensor or array of sensors installed in the target area, peak amplitude of motion is quickly estimated, and the warning is issued if required. In this way, there is no need to estimate the magnitude and epicentral distance (Colombelli et al., 2015). In recent years, many measures have been taken to use a combination of on-site and regional warning in an attempt to obtain earlier warning and reduce the blind zone extent (warning free zone) (Allen et al., 2009).

As a whole, estimation of earthquake source parameters including magnitude, epicentral distance and peak ground motion is of great importance in all EEW systems. Besides, there is an uncertainty between rapidness and accuracy to estimate EEW parameters. Therefore, the parameters estimation updates after first early warning to obtain more accurate and reliable estimation. This process often starts in one or two seconds after triggering the P-wave and continues for longer time windows. Three, four or longer time windows are often more reliable for large earthquakes, which have long rupture time duration.

The method 2-second $B-\Delta$ is one of the methods used by Japan EEW system to estimate epicentral distance in a single station (Odaka et al., 2003; Noda et al., 2012). In this method, epicentral distance can be quickly estimated considering the characteristics of the initial seconds of P-waves envelope on a single station. Moreover, given the absolute values of the amplitudes recorded in the initial few seconds after the P-wave arrival, an exponential function is fitted as $B \times t \times e^{-A \times t}$. For any vertical component of seismic acceleration waveform, A and B parameters are calculated by the least squares method. The constant B (gal/s) indicates the slope of the initial part of envelope that is decreased with distance from epicenter, so that a magnitude independent linear relation is formed between $log(B)$ and $-log(\Delta)$ to estimate the epicentral distance. Δ per kilometer denotes the epicentral distance of the earthquake. Changes in amplitude envelope arising from scattering during

the wavefront expansion lead to the negative correlation between B and Δ (Tsukada et al., 2004). The constant $(1/s)$, takes a negative value wherever amplitudes have increased over time, which is usually observed in large magnitude earthquakes. It takes positive value wherever the amplitudes has grown rapidly at first and decreased gradually that is observed in small earthquakes (Odaka et al., 2003). The maximum value for the exponential function for $A > 0$ is B/Ae (e is the base of natural logarithms) (Odaka et al., 2003). This method is used to estimate the single station epicentral distance by EEW system of Japan Meteorological Agency (JMA) (Kamigaichi, 2004; Kamigaichi et al., 2009; Noda et al., 2012), where the earthquake magnitude is estimated by using an empirical attenuation relation that depends on the maximum amplitude of window and the epicentral distance logarithm (Odaka et al., 2003). In this study, new parameters are proposed based on characteristics of the initial seconds of P-waves envelope so that the earthquake magnitude and PGA amplitude together with earthquake epicentral distance can be estimated with higher precision (in case of large earthquakes).

2 Database

This study is conducted by using 226 vertical component of bore-hole acceleration waveforms of Japanese KiK-net (http://kyoshin.bosai.go.jp) with a sampling frequency of 100 Hz, belongs to the National Research Institute for Earth Science and Disaster Prevention (NIED). Only waveforms whose Signal-to-Noise Ratio (SNR) is greater than 10 were selected among all the existing waveforms during 2000-2015. All waveforms are related to earthquakes with M_{JMA} magnitudes between 3 and 7.2, and epicentral distances between 10 and 50 km and depths less than 30 km. The number of earthquakes and their distribution are listed in Table 1.

3 Epicentral Distance Estimation

Estimating the epicentral distance through B – Δ method includes the following processes: (1) The mean and trend values are removed from signals, then a Butterworth band-pass filter with 10-20 Hz frequency band is applied (Noda et al., 2012) to the understudy waveforms, because the radiation pattern of high-frequency ground motions seems to be isotropic (Liu and Helemberger, 1985; Kobayashi et al., 2014). (2) A 4-second time window is extracted from the initial portion of P-waves and a cosine taper weighted 0.03 is applied to reduce the harmful effects of signal edges two ends. For records polluted by shear S-wave within initial 4 s of waveforms, only P-wave part of waveforms up to the S-wave arrival times have been considered. (3) The absolute values logarithm related to acceleration amplitudes is calculated as follows. At this stage, a partial amount is added to all amplitudes to avoid problems arisen from zero amplitudes. (4) The exponential

Table 1. Accelerogram distribution according to distance (km) and magnitude (M_{JMA}).

Magnitude/Distance interval	10-20	20-30	30-40	40-50	Summation	Number of events
3-3.9	9	12	16	28	65	17
4-4.9	3	11	15	18	47	12
5-5.9	7	13	20	25	65	15
6-6.9	3	6	7	10	26	16
7-7.2	2	4	6	11	23	7
Summation of each column	24	46	64	92	226	67

function $y = B \times t \times e^{-A \times t}$ in logarithmic form $ln(y/t) = ln(B) - At$ is fitted to the absolute values logarithm related to acceleration amplitudes, and B and A parameters are extracted by using the least squares method. Mentioned approach has shown in Figure 1 for two earthquake acceleration amplitude records. Figure 1a belongs to a small earthquake occurred in year 2015 with magnitude of 3.5 (M_{JMA}), epicentral distance of 47 (Km) with a positive value of A, and Figure 1b is related to a large earthquake in year 2011 with magnitude of 6.7 (M_{JMA}), epicentral distance of 23 (Km) with a negative value of A. At last, rational time, T_r, is defined by using the exponential function fitted on acceleration envelope in the 4-second time window as follows:

$$T_r = \frac{t_{max}}{t_{max} - t_e} \quad (1)$$

where t_{max} denotes the time whenever the amplitude envelope curve of strong ground motion reaches its maximum value and t_e denotes the time whenever the amplitude envelope curve reaches $1/e$ of its maximum value. Odaka et al. (2003) showed that B parameter, without any earthquake magnitude dependency, is a function of epicentral distance and the effects of the earthquake source (e.g. directivity effect) and even the local site effects in stations are not considered in $B - \Delta$ method. In this study, $B \times T_r$ parameter is used instead of B to show a better correlation between growth of envelope curves of the initial portion of signals and epicentral distances for large earthquakes ($M > 6$).

Figure 2 shows the scattering for T_r measurements against earthquake magnitudes and A parameter values for the understudy database. It shows that T_r values are clearly increased for earthquakes with negative values of A (large earthquakes) while it is close to constant value of 1 for other earthquakes. Comparing T_r values and earthquake magnitudes indicates that for some T_r measurements, rational time values are increased with earthquake magnitudes showing the dependency of this non-

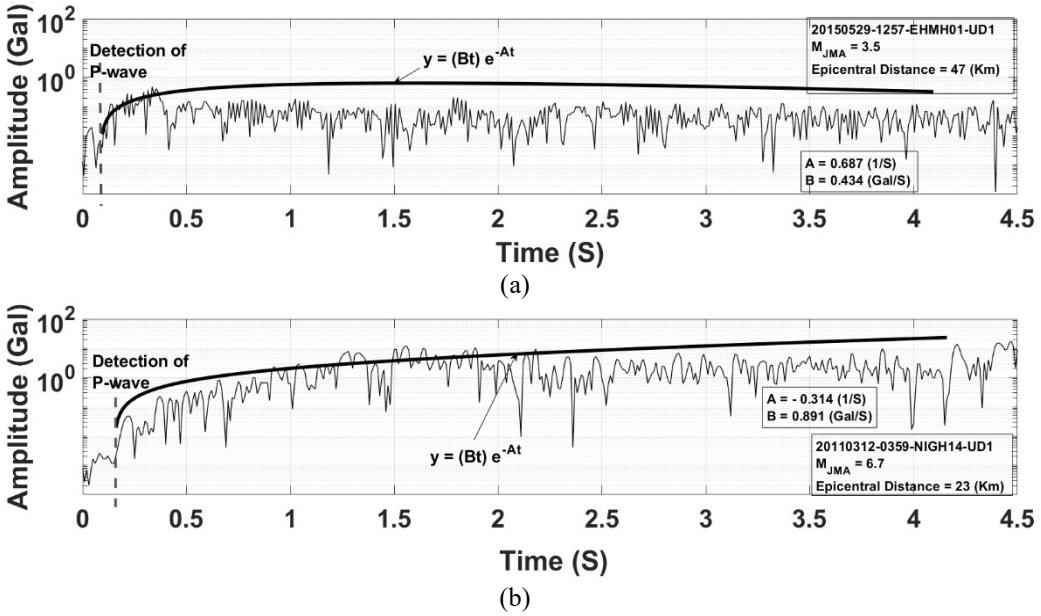

Figure 1. Amplitude envelope curve with the function of $y = B \times t \times e^{-A \times t}$ on a 4-second initial P-wave envelope window by using $B - \Delta$ method (a) for an earthquake in 2015, epicentral distance of 47 Km and magnitude of 3.5, and (b) for an earthquake in 2011, epicentral distance of 23 Km and magnitude of 6.7.

dimensional parameter on source specifications and parameters. Possible causes of increasing some T_r values seems to be dependent on radiation pattern and source function, etc. Finite-fault source model's characteristics such as directivity, rupture time duration and rupture velocity effects do not play an important and key role in T_r measurements for small earthquakes (in point source model). Against, for larger earthquakes, differences in radiation pattern and source function may be caused to increase T_r measurements with magnitude. Although, proposed relationships and methods in this study are obtained for less than 50 km distances, we plotted the T_r measurements with distances between 10 and 150 km for better interpretation of this parameter with magnitude shown in Figure 2a. In this study, only, rational time parameter effects on epicentral distance estimation has studied and more investigations need an exact description of large earthquakes P-wave envelope features.

In addition to evaluating the values of B, the values of $B \times T_r$ are also evaluated to estimate epicentral distance more precisely. For this purpose, the values of $log\ (\Delta)$ against the values of $log(B)$ and $log(B \times T_r)$ are depicted in Figure 3 and the best line is fitted by using the least squares method. Empirical relationships to evaluate epicentral distance are defined by using both methods of B – Δ (Equations 2 and 4) and $B \times T_r$ – Δ (Equations 3 and 5) as follows for two different magnitude range:

$$log(\Delta) = -0.963\ log(B)\ + 1.233\ (\pm 0.54) \quad (3 \leq M_{JMA} \leq 7.2) \tag{2}$$

$$log(\Delta) = -0.965\ log(B \times T_r) + 1.384\ (\pm 0.40) \quad (3 \leq M_{JMA} \leq 7.2) \tag{3}$$

$$log(\Delta) = -0.780\ log(B) + 1.323\ (\pm 0.53) \quad (6 \leq M_{JMA} \leq 7.2) \tag{4}$$

$$log(\Delta) = -0.728\ log(B \times T_r) + 1.586\ (\pm 0.32) \quad (6 \leq M_{JMA} \leq 7.2) \tag{5}$$

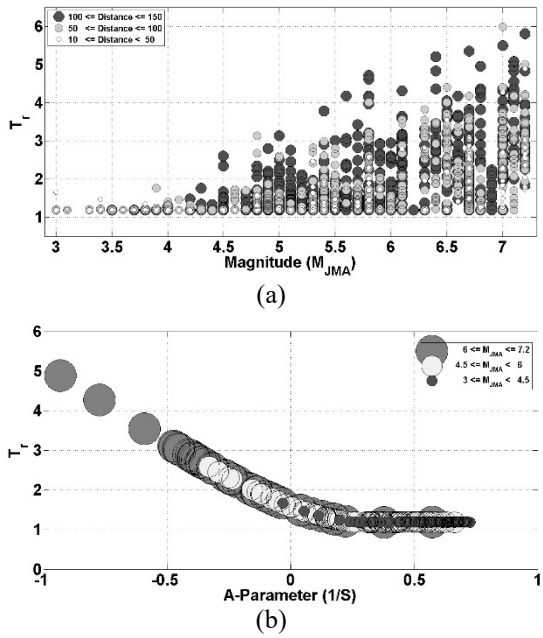

Figure 2 Illustration of T_r against (a) magnitude for epicentral distances of less than 150 km, and (b) A parameter for epicentral distances of less than 50 km and magnitudes of 3 to 7.2 M_{JMA}.

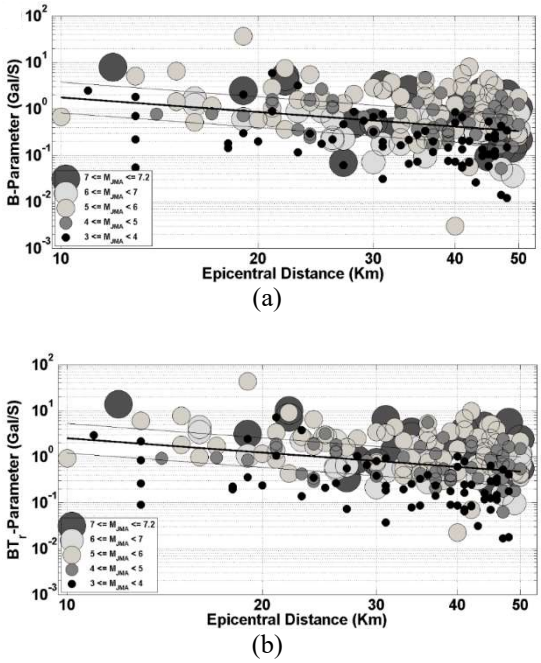

Figure 3 Linear regression (a) between $log(\Delta)$ and $log(B)$ and (b) between $log(\Delta)$ and $log(BT_r)$ for magnitudes of 3 to 7.2 M_{JMA}.

According to obtained standard deviation values, the second method ($B \times T_r - \Delta$) shows a better accuracy to estimate the epicentral distance of large earthquakes ($M > 6$). The results are indicative of the fact that parameter T_r reduces the effects of the earthquake source parameters on epicentral distance estimation.

4 Magnitude Estimation

Heidari (2016) proposed a magnitude-scale relationship as $M = \alpha \log(A \times P_{max}) + \beta \log(B) + \gamma$ based on acceleration records for 17 earthquakes happened in Iran. Generally, in original definition of curve function, A^{-1} is the required time for curve to reach its maximum value for positive A values (i.e. B/Ae). Heidari (2016) changed the definition of A^{-1} parameter as a required time for curve $B \times t \times e^{-A \times t}$ to reach $1/e$ of its maximum value to avoid negative values of A for large magnitude earthquakes.

In mentioned magnitude-scale relation, the distance-dependency parameter B is considered for normalizing distance effects, because Heidari (2016) used the waveforms with epicentral distances up to 150 km.

In this study, in order to estimate the earthquake magnitude based on characteristics of the envelope curve fitted on amplitudes of strong ground motion within the first few seconds, the area under the envelope curve is considered during $t_{max} - t_e$. In this study, it is assumed that the under envelope curve area is affected by epicentral distance before t_e and by environmental characteristics such as t_{max} waves post diffraction and scattering. Therefore, magnitude scale parameter, S_a $(gal.s)$ is calculated for each waveform recorded in the station by using maximum amplitude envelope curve of the initial P-waves (P_{max}) as:

$$S_a = \left(t_{max} - t_e\right) \times P_{max} \quad (6)$$

As shown in Figure 4 (Equation 7), the logarithm of S_a is well correlated with M_{JMA} magnitude and linear trends are formed as follows:

$$M = 1.939\, log(S_a) + 4.126\ (\pm 0.77) \quad (3 \leq M_{JMA} \leq 7.2) \quad (7)$$

where M is the magnitude extracted from envelope curve independent of the initial portion slope of P-waves as the most important part of the curve affected by epicentral distance. Besides, in this method, distance effect on second part of the amplitude curve is neglected for short distances of less than 50 km. Although the earthquakes magnitude estimation greater than 7 is saturated in the 4-second time window (Zollo et al., 2006), the main point is that a warning alarm could be issued, if a large earthquake is expected.

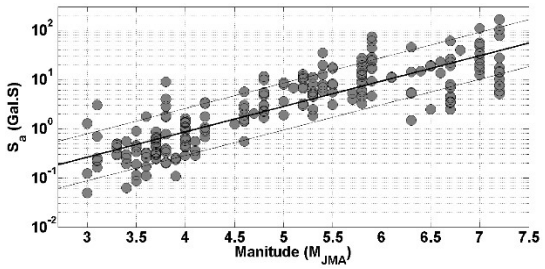

Figure 4 Linear regression between S_a and magnitude for less than 50 km distances and magnitudes of 3 to 7.2 M_{JMA} .

5 PGA Estimation

At last, A and B parameters obtained by using $B - \Delta$ method in 4-second time window of initial P-waves are used to estimate PGA. Figure 5a shows two clusters almost different from each other between $log(\frac{B}{A})$ (for positive value of A as a feature of small earthquakes) and $log(PGA)$ (per gal) and between $log(\frac{B}{|A|})$ (for negative value of A as a

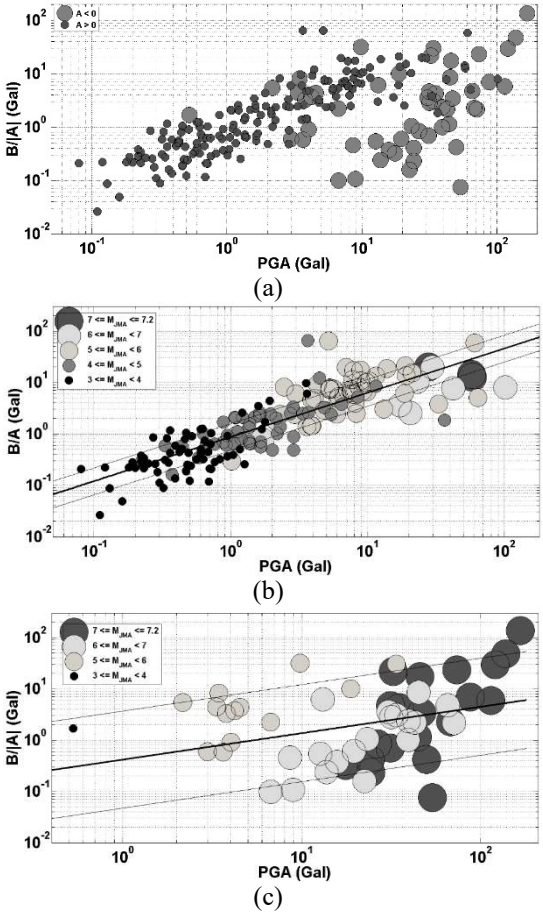

Figure 5 (a) $B/|A|$ values against *PGA* and linear regression (b) between $log(\frac{B}{A})$ and $log(PGA)$, for $A > 0$ (c) between $log(\frac{B}{|A|})$ and $log(PGA)$ for $A < 0$.

feature of large earthquakes) and $log(PGA)$. It is assumed that the maximum strong ground motion shows a direct correlation with $\frac{B}{A}$ parameter. This parameter is a function of earthquake magnitudes and distances, potentially and indirectly by employing A and B parameters. There is a clear and appropriate trend between $log(\frac{B}{A})$ and $log(PGA)$. However, it does not observe a high quality and tangible linear pattern between $log(\frac{B}{|A|})$ and $log(PGA)$. It should be noted that this almost large scattering may be the result of fewer number of large earthquakes against small and moderate earthquakes numbers, in this study. According to Figure 5, the following relationships are obtained for $A > 0$ (Equation 9, Figure 4b) and $A < 0$ (Equation 10, Figure 4c) at less than 50 km distances:

$$log(PGA) = 1.163\, log\left(\frac{B}{A}\right) + 0.074\ (\pm 0.41) \quad (3 \le M_{JMA} \le 7.2, A > 0) \tag{8}$$

$$log(PGA) = 1.940\, log\left(\frac{B}{|A|}\right) + 0.738\ (\pm 1.56) \quad (3 \le M_{JMA} \le 7.2, A < 0) \tag{9}$$

Although PGA value is the key parameter in on-site (single station) EEW systems, the warning can be issued when PGA exceeds from a threshold value. Providing a robust database in case of large earthquake, has deferred the future to investigate for a more reliable relationship between $log(\frac{B}{|A|})$ and $log(PGA)$.

6 Conclusions

This study aims to present an improved relationship for estimation of epicentral distance. In addition, two linear relationships is presented for magnitude and PGA estimation in the 4-second window of the initial portion of P-waves based on envelope curve features of strong ground motion through $B - \Delta$ method proposed by Odaka et al. (2003). First, a new non-dimensional parameter T_r is proposed by using the curve characteristics proposed in $B - \Delta$ method as $B \times t \times e^{-A \times t}$. Generally, T_r measurements increase with magnitude shown in Figure 2a. This parameter is independent of the earthquake epicentral distance (at least for the range of less than 50 km in this study), and it may be one of the major characteristics of the rupture (such as radiation pattern and rupture velocity). However, the role of path effects including geometrical spreading and intrinsic attenuation is not separated. Besides T_r correlates with parameter A (related to magnitude) and the larger values of T_r is obtained for

negative values of A (large earthquakes). The standard deviation of $B \times T_r - \Delta$ improved relation in 4-second time window for earthquakes greater than 6 is calculated ± 0.32 against ± 0.53 by $B - \Delta$ method, which may be due to the modification of some source effects on the slope of P-waves initial portion. The numerical results show that by inserting T_r in algorithm of $B - \Delta$ method and using $B \times T_r - \Delta$ in a 4-second time window, epicentral distance of large events could be more carefully estimated from slope of the initial portion of acceleration envelope curve. Then, the events magnitude is estimated by parameter S_a that is obtained from an area portion lying under acceleration envelope curve of the 4-second time window, where it includes two effective parameters, maximum amplitude of envelope curve and time difference between maximum and $1/e$ of maximum envelope curve amplitude. Magnitude relationship standard deviation is obtained ± 0.77 magnitude unit.

Therefore, the new method for quick magnitude estimation in a 4-second time window of P-waves initial portion is considered to be reliable. At last, a new relationship is stablished to calculate PGA. For this purpose, B parameter related to epicentral distance and A parameter related to magnitude are used and a linear relationship is formed between $log(PGA)$ and logarithm of B to absolute value of A ratio (for negative values of A) and B to A ratio (for positive values of A) per gal. Standard deviation of the estimated PGA is obtained ±1.56 (for negative values of A) and ±0.41 (for positive values of A). In Table 2, some observed values collected in Japan Meteorological Agency's catalog have compared to estimated EEWS parameters values from Equation (3) for distance, Equation (7) for magnitude, and eq. 8 for PGA. The numerical results show that using new form of equations to estimate source parameters (magnitude and epicentral distances), and PGA can reliably be used in on-site early warning systems. Estimation of magnitude, epicentral distance and peak ground motion based on P-waves initial part is the most important function of EEW systems. As a result, these relations can also be used in regional networks.

Table 2. Comparison of observed and estimated values of magnitude, distance and PGA, for selected events. Observations are made by JMA and estimated values are based on Equation (3) for distance, Equation (7) for magnitude, and Equation (8) for PGA.

Event (Y,M,D)	$Magnitude_{obs}$ (M_{JMA})	$MagnitudeE_{est}$ (M_{ec})	$Distance_{obs}$ (Km)	$Distance_{est}$ (Km)	PGA_{obs} (Gal)	PGA_{est} (Gal)
2011,03,12	6.7	6.6	23	11	31.7	41.42
2012,04,29	5.8	5.9	20	21	4.23	5.47
2012,04,29	5.8	5.4	36	48	4.03	4.52
2012,04,29	5.8	5.6	49	52	2.3	3.2
2015,02,09	3.3	3.5	41	31	0.52	1.05
2015,02,09	5.5	5.6	45	38	8.67	13.66
2015,02,09	3.5	3.5	47	45	0.71	0.7
2015,05,30	4.8	4.8	26	18	3.35	3.39
2015,07,04	5.7	5.3	46	49	2.39	3.22
2015,07,29	4	3.4	42	41	0.88	0.77
2015,08,23	4.2	4.2	23	55	0.76	0.68
2015,08,23	4.2	5.1	26	20	2.13	2.6
2015,09,08	4	4.4	29	30	1.35	1.67
2015,09,08	4.6	4.4	50	43	0.94	1.07
2015,11,04	4.1	3.6	38	43	1.36	0.81

7 Data and resources

The data used in this study were extracted from KiK-net of the National Research Institute for Earth Science and Disaster Prevention (NIED; http://kyoshin.bosai.go.jp, last accessed February 2016). The tools used in the current study include: Seismic Analysis Code software (SAC; http://ds.iris.edu/ds/nodes/dms/software/downloads/sac/, last accessed July 2013) for the data processing and Matrix Laboratory (MATLAB v.R2013anew; www.matworks.com/products/, last accessed February 2016) software for preparing figures.

References

Allen, R. M., Gasparini, P., Kamigaichi, O., and Böse, M., 2009, The status of earthquake early warning around the world: an introductory Overview: Seismological Research Letters, **80**(5), 682-693, doi:10.1785/gssrl.80.5.682.

Colombelli, S., Caruso, A., Zolla, A., Festa, G., and Kanamori, H., 2015, A P wave-based on-site method for earthquake early warning: Geophysical Research Letters, **42**(5), 1390-1398, doi:10.1002/2014GL063002.

Espinosa-Aranda, J. M., Cuellar, A., Garcia, A., Ibarrola, G., Islas, R., Maldonado, S., and Rodriguez, F. H., 2009, Evolution of the Mexican seismic alert system (SASMEX): Seismological Research Letters, **80**(5), 694–706. doi:10.1785/gssrl.80.5.694.

Espinosa-Aranda, J. M., Jimenez, A., Ibarrola, G., Alcantar, F., Aguilar, A., Inostroza, M., and Maldonado, S., 1995, Mexico City seismic alert system: Seismological Research Letters, **66**(6), 42–53, doi:10.1785/gssrl.66.6.42.

Heidari, R., 2016, Quick estimation of the magnitude and epicentral distance using the P wave for earthquakes in Iran: Bulletin of the Seismological Society of America, **106**(1), 225-231, doi:10.1785/0120150090.

Horiuchi, S., Negishi, H., Abe, K., Kamimura, A., and Fujinawa, Y., 2005, An automatic processing system for broadcasting earthquake alarms: Bulletin of the Seismological Society of America, **95**(2), 708–718, doi:10.1785/0120030133.

Hoshiba, M., Iwakiri, K., Hayashimoto, N., Shimoyama, T., Hirano, K., Yamada, Y., Ishigaki, Y., and Kikuta, H., 2011, Outline of the 2011 off the pacific coast of Tohoku earthquake (Mw 9), earthquake early warning and observed seismic intensity: Earth Planets and Space, **63**(7), doi:10.5047/eps.2011.05.031.

Kamigaichi, O., 2004, JMA earthquake early warning: Journal of Japan Association for Earthquake Engineering, **4**(3), 134–137, doi:10.5610/jaee.4.3_134.

Kamigaichi, O., Saito, M., Doi, K., Matsumori, T., Tsukada, S., Takeda, K., Shimoyama, T., Nakamura, K., Kiyomoto, M., and Watanabe, Y., 2009, Earthquake early warning in Japan: Warning the general public and future prospects: Seismological Research Letters, **80**(5), 717–726, doi:10.1785/gssrl.80.5.717.

Kuyuk, H. S., and Allen, R.M., 2014, Designing a network-based earthquake early warning algorithm for California, Elarm S-2: Bulletin of the Seismological Society of America, **104**(1), 162-173, doi:10.1785/0120130146.

Kobayashi, M., Takemura, S., and Yoshimoto, K., 2014, Distortion of the apparent P-wave radiation pattern. In abstract of the seismological society of Japan: Fall Meeting, 24-26.

Liu, H. L., and Helmberger, D. V., 1985, The 23:19 aftershock of the 15 October 1979 imperial valley earthquake, More evidence for an asperity: Bulletin of the Seismological Society of America, **75**, 689-708.

Nakamura, Y., 1988, On the urgent earthquake detection and alarm system (UrEDAS), Proceedings of 9th World Conference of Earthquake Engineering, **7**, 673–678.

Nakamura, Y., 2004, UrEDAS, urgent earthquake detection and alarm system, now and future, Proceedings of 13th World Conference of Earthquake Engineering, August 2004, paper no. 908.

Noda, S., Yamamoto, S., and Sato, S., 2012, New method for estimation earthquake parameters for earthquake early warning system, Q. Rep. Railway. Tech. Res. Inst., 53(2), 102-106, doi:10.2219/rtriqr.53.102.

Odaka, T., Ashiya, K., Tsukada, S., Sato, S., Ohtake, K., and Nozaka, D., 2003, A new method of quickly estimating epicentral distance and magnitude from a single seismic record: Bulletin of the Seismological Society of America, **93**(1), 526–532, doi:10.1875/0120020008.

Satriano, C., Elia, L., Martino, C., Lancieri, M., Zollo, A., and Iannaccone, (2010) PRESTO, the earthquake early warning system for Southern Italy: Concepts, capabilities and future perspectives. Soil Dynamics and

Earthquake Engineering, **31**(2), 137-153, doi:10.1016/j.soildyn.2010.06.008.

Tsukada, S., Odaka, T., Ashiya, K., Ohtake, K., and Zozaka, D., 2004, Analysis of the envelope waveform of the initial part of P-waves and its application to quickly estimating the epicentral distance and magnitude: Zisin, **56**, 351-361.

Wu, Y. M., and Teng, T. L., 2002, A virtual subnetwork approach to earthquake early warning: Bulletin of the Seismological Society of America, **92**(5), 2008–2018. doi:10.1785/0120010217.

Wu, Y. M., and Zhao, L., 2006, Magnitude estimation using the first three seconds P-wave amplitude in earthquake early warning: Geophysical Research Letters, **33**, doi:10.1029/2006GL026871.

Zollo, A., Lancieri, M., and Nielsen, S., 2006, Earthquake magnitude estimation from peak amplitudes of very early seismic signals on strong motion records: Geophysical Research Letters, **33**, doi:10.1029/2006GL027795.